

**Military Technical College  
Kobry El-Kobbah,  
Cairo, Egypt.**



**18<sup>th</sup> International Conference  
on Applied Mechanics and  
Mechanical Engineering.**

## **MODELING OPEN-CELLED ALUMINUM FOAMS STRUCTURE USING 3-D VORONOI DIAGRAM**

A. M. Fathy<sup>1</sup>, M. H. Abdelshafy<sup>2</sup> and M. R. A Atia<sup>3</sup>

### **ABSTRACT**

Three dimension (3-D) Voronoi diagram is used to model open-celled Aluminum foam structures. This model simulates the compression response of open-celled Aluminum foam. Models of aluminium foam with different relative density and different cell regularities are used in simulations using ABAQUS. Finite element analysis (FEA) has been carried out to simulate the compression process on Aluminum Foam up to 15% strain. Stress-strain curve relation is predicted for each model. The results show good agreement with published experimental and mathematical modeling works. The developed model could be accepted as a virtual platform for modeling open-celled Aluminum foam structure.

### **KEYWORDS**

Open-celled Aluminium foam; Computer simulations; Finite element modelling

---

<sup>1</sup> Graduate student, Dept. of Mech., AASTMT, Cairo, Egypt.

<sup>2</sup> Egyptian Armed Forces.

<sup>3</sup> Associate professor, Dept. of Mech., AASTMT, Cairo, Egypt.

## INTRODUCTION

Open-celled Aluminum foams are widely used because of their high mechanical properties relative to their low density and energy absorption characteristics. The lightweight design philosophy and energy absorption characteristics are important in several applications, such as automotive, aerospace, shipbuilding industries and military applications. Modern aircraft used the sandwich structure of Aluminum foam or paper-resin honeycombs for their lightweight and high stiffness [1]. The same technology has spread to automotive applications in which reducing weight is desirable and increasing vehicle passive safety performance is mandatory [2]. Modern boats and ships use a sandwich structure forming [3]. Aluminum foam is used in military applications in mitigation of blast effects [4] and as sacrificial cladding material, which reduce the blast air-blast loading [5]. Moreover, it's used in sound absorption applications [6].

Researchers used different methods to obtain Aluminum foam characteristics such as experimental, mathematical modeling and simulation. Experimental methods [7] are favorable and reliable in many cases. However, they are costly and time-consuming; therefore, it is not suitable for the early design stage. Mathematical modeling methods depend on exact solution starting from basic principles [8] and [9]. They are not able to take into account all characteristics and may be simplified using many assumptions, which reduce their accuracy. Thus, practically, they cannot describe efficiently all Aluminum foam characteristics. Simulations of virtual model are commonly used in early design stages ([10], [11],[12] and [13]) because designers can do them repeatedly on different designs with low-cost and short time. Moreover, the closer the model to reality, the designers get better results.

The aim of the present work is to build a virtual model that able to capture the real characteristics of open-celled Aluminum foams. The predictions of this model will be validated with the corresponding measurements of other investigators ([14], [7], [8], and [9]). The present work is divided into three main sections. The first section presents the steps of construction of the improved 3D Voronoi model for Aluminum foam structure. The second is a finite element modeling in which the developed structure model is transformed to finite element program ABAQUS. Finally, this model is tested in compression to obtain stress-strain curve and validate the results with those obtained from previous experimental and mathematical modeling researches.

## SOLID MODELING

The suggested structural model consists of three parts: upper plate, lower plate, and Aluminum foam structure as shown in (Fig. 1). Voronoi diagram is used to model Aluminum foam structure; its construction is based on Voronoi seeds distribution, which defines Voronoi diagram regularity. The Number and size of cells in Voronoi diagram represent the pores of the Aluminum foam.

### Voronoi Diagram

Voronoi diagram is defined as partitioning of a plane into regions based on distance to points in a specific subset of the plane [15]. This set of points is called seeds. These seeds should be specified beforehand. As shown in (Fig. 2), for every seed

there is a corresponding region consisting of all points closer to this seed than to any other. These regions are called Voronoi cells. Voronoi edge is either a line segment connecting two Voronoi vertices or a ray starts from a Voronoi vertex in the case of boundary edges. As shown in (Fig. 3) rays are trimmed by model planes.

### Defining voronoi regularity

The Voronoi diagram can be generated in different regularities starting from completely irregular up to completely regular. Zhu et al. [8] defined the level of regularity  $\delta$  as:

$$\delta = \frac{d}{h} \quad (1)$$

where  $d$  and  $h$  are the maximum distances between the neighboring seeds in the cases of irregular and regular Voronoi diagram, respectively, with the same volume  $V$  and the number of seeds  $N$ . The distance  $h$  is given by [8]:

$$h = \frac{\sqrt{6}}{2} \left( \sqrt[3]{\frac{V}{\sqrt{2} N}} \right) \quad (2)$$

### Generating voronoi seeds

As mentioned before, Voronoi seeds must be defined first to generate the Voronoi diagram. Simple sequential inhibition process (SSI) [16] was used to produce random points and get irregular Voronoi cells. In SSI process, points in space are generated based on a completely random process described by the Poisson distribution. After every point is generated, its distances with respect to the previous ones are evaluated. If none of these distances are greater than a threshold value  $d$  then, the point is kept. Otherwise, it is eliminated. The process continues until points are generated. Figures 4a and 4b show seeds generated regularly and generated by SSI method in 3-D space, respectively.

### Model size and number of cells in the model

Ashby et al. [17] stated that the open-cell aluminum foams are available with a pore densities of 10, 20, 40 pores per inch according to the manufacturer. Thus, it can be assumed that the average cell density is equal to 24 cells per inch. Sotomayor [10] presented an analysis of the number of nuclei ( $N$ ) required to generate ( $k$ ) Tetrakaidecahedron cells along the border of a unit cube as:

$$N = (k + 1)^3 + k^3 \quad (3)$$

For 0.25 inch,  $k$  equals 6 cells and  $N$  will be 559 nuclei. Andrews et al [18] have experimentally studied the effect of the specimen size on the compression response of aluminum foams. They suggested that a ratio of the specimen size to cell size should be not less than 6 to predict the elastic modulus and present a tolerable difference in the prediction of the plastic collapse strength of aluminum foams. For a regular foam, Sotomayor et al. [19] stated that a ratio of the specimen size to the cell size of 6 corresponds to  $n = 341$  cells for 0.25 inch cube. 559 cells in 0.25 inch cube are used to achieve 24 cells per inch and to keep the ratio of the specimen size to cell more than 6.

Beam section with a constant circular profile is assigned for all the line features created using Voronoi diagram and it is called strut. In fact, this cross section is varying. Such constant idealization through all the beam length is acceptable when relative densities is less than 10% [20]. Zhu et al. [12] used a formula to calculate the value of the strut diameter, which depends on the relative density of the foam. This formula is used in the present work and is given by:

$$\bar{\rho} = \rho^* / \rho_s = \left( \frac{1}{V} \right) \sum_{i=1}^n \frac{\pi}{4} d_i^2 l_i \quad (4)$$

where  $\rho^*$  is the density of foam,  $\rho_s$  is the density of solid material forming foam,  $d$  is the diameter of struts forming foam,  $l$  is the length of struts,  $V$  is the volume of foam and  $n$  is number of struts.

The thickness of either upper or lower plate is assumed to be 1% of the thickness of Aluminum foam structure [19]. In present research, 0.25 inch is the thickness of suggested Aluminum foam model. Thus, the thickness of upper and lower plate is equal 0.0025 inch. The areas of the plates must be slightly greater than the upper and lower surface areas of Aluminum foam structure to guarantee contact during compression.

### Creation of the model

In the present work, 3-D Voronoi models with different relative density  $\bar{\rho} = \{1\%, 3\%, 5\%, 7\%, 9\%\}$  and three different regularities  $\delta = \{50\%, 70\%, 80\%\}$  are considered. For each regularity, 20 models were generated by a different random distribution of seeds. These combinations generated 300 models for regularity less than 100%. A C++ program was developed to generate and draw these models automatically. This program encapsulates TetGen library [21] to get Voronoi cells.

## FINITE-ELEMENT MODELING

For the present case study, the finite-element package ABAQUS/Standard is used. In the pre-processing stage, the Voronoi diagram geometry, in DXF format, is obtained by the developed model generation program. Then DXF format is transformed to IGS format using the Autodesk/Inventor package. Then, IGS file format is imported to ABAQUS to form foam structure. Foam structure is merged with upper and lower plates to form sandwich structure.

Al-6061-T6 was used as a base material forming struts and face-sheets. It was modelled as an elastoplastic material. The elastic region was defined by isotropic hardening model. The elastic properties are completely defined by  $E$  and  $\nu$ . For Al-6061-T6  $E = 68.9 \text{ GPa}$  and  $\nu = 0.33$  [22]. The plastic region was defined by Johnson-Cook model [23]. Its coefficients are summarized in Table 1. **Jacob et al.** [24] produced these coefficients and validated them with the corresponding measurements.

Kanahashi et al. [14] stated that the compressive deformation behavior of open-celled Aluminum foams exhibits negligible strain rate dependence. Thus,  $0.15 / \text{s}^{-1}$  is set as the strain rate during simulation to ensure the convergence of solution.

Boundary conditions were applied to the upper and lower plates. The upper plate and the lower plate were allowed to move only in one direction perpendicular to each other. Equal and opposite displacements ( $\alpha_1$  and  $\alpha_1$ ) were applied to plates in z direction as shown in Fig. 5.

Voronoi ligaments were discretized with 3-node quadratic beam elements (B32) in ABAQUS. Quadratic interpolation was used. Voronoi diagram contains very small edges specially by increasing irregularity. These small edges cause solution divergence if number of elements per edge become more than two elements. To avoid the divergence of solution due to small ligaments, especially in high irregularities models, two elements per ligaments were used [10]. The upper and lower plates were discretized with four-node Shell elements. They were generated to coincide with nodes in the beam elements. A total number of elements in all models were varied from 11,000 to 12,000. The general static method was selected to capture changes in reaction forces and displacement of upper and lower plates.

In the post-processing stage, at every step of the solution, forces at every element of lower plate were added to form the total reaction force. Displacements of lower plate and upper plate were added to form total displacement. In order to draw stress-strain relation, total reaction force was divided by cross section area of aluminum foam cube to form stress [19]. Displacement was divided by the original length of aluminum foam cube to form strain.

## RESULTS AND VALIDATION

In this section, the obtained results from the proposed model will be presented then they will be compared with published works ([14], [7], [8] and [9]).

### Results

Based on the simulations of the developed model, the obtained engineering stress for all foams for present study is normalized by yield stress  $\sigma_{ys}$  and relative density  $\bar{\rho}$  to the power 1.5 [19]. The normalized stress is given by:

$$\bar{\sigma} = \frac{\sigma}{\sigma_{ys} \cdot \bar{\rho}^{1.5}} \quad (5)$$

Stress-strain curves were evaluated for the different relative density and regularity. Fig. 6 is an example of these stress-strain curves. As shown in Fig. 6, Stress-strain curves are able to capture the normal behaviour of open-celled Aluminum foams during compression up to 15% strain. They are able to capture elastic region and plastic collapse region.

### Model validation using stress-strain curve

The obtained results are validated using available experimental results. Kanahashi et al. [14] measured stress-strain relations of open-celled Aluminum foam at relative density 9% for both quasi-static and dynamic strain rates, respectively. They used specimens with different cells sizes (10, 20, 40 ppi). They used Al 6101-T6 as a base material, which is different from the base material used in this research. To compare simulation results presented in this paper with experimental results of reference [14],

both stress-strain curves are normalized with equation (5) [19]. As shown in Fig. 7, the normalized stress-strain curves that obtained from simulations are bounded by the upper and lower limit of normalized stress-strain curves measured by Kanahashi et al.[14].

### **Model validation using normalized modulus of elasticity and plastic collapse strength**

The elastic region was validated using normalized modulus of elasticity ( $E^*/E_s$ ) of Voronoi structures. The obtained modulus of elasticity ( $E^*$ ) is normalized by modulus of elasticity of base material forming foam  $E_s$ . The mean of normalized modulus of elasticity of different regularities was compared with those obtained from three different previous works ([7], [8] and [9]) at different relative density as shown in (Fig. 8). The normalized modulus of elasticity for different relative density is bounded by the results of references ([7], [8] and [9]). Similarly, the plastic collapse region was validated using normalized plastic collapse strength ( $\sigma_{pl}^*/\sigma_{ys}$ ) of Voronoi structures. In Fig. 9, the results were compared with those published in references [7]. The obtained results show the same trend of increasing of normalized plastic collapse strength with the increase of relative density yet with slightly different rate. These comparisons between the obtained results of simulations and those published in previous references showed a good agreement. Therefore, this means that the developed model is a suitable virtual platform for modeling Aluminum foam.

### **CONCLUSION**

- 3-D Voronoi models were developed with different relative density  $\bar{\rho} = \{1\%, 3\%, 5\%, 7\%, 9\%\}$  at different regularities  $\delta = \{50\%, 70\%, 80\%\}$ .
- Al-6061-T6 was used as a base material forming struts. It was modelled as an elastoplastic material.
- A finite element analysis was carried out using these models to evaluate stress-strain curves during compression.
- Results show good agreement between the obtained stress-strain curves of suggested model and published experimental works.
- Results show good agreement between the obtained modulus of elasticity of suggested model and published works.
- Results show good agreement between the obtained plastic collapse strength of suggested model and published works.
- The developed model could be accepted as a virtual platform for modeling open-celled Aluminum foam structure.

### **REFERENCES**

- [1] G. Yao, H. Luo, and Z. Cao, "The Manufacturing Technology of Aluminum Foam Material and Some Special Equipments", No. Icmsa, pp. 869–874 (2015).
- [2] J. Banhart, "Aluminium Foams for Lighter Vehicles", Int. J. Veh. Des., Vol. 37, No. 2–3, pp. 114–125 (2005).
- [3] G. Marsh, "Material Trends for Frp Boats", Reinf. Plast., Vol. 47, No. 9, pp. 23–34 (2003).

- [4] Y. Su, C. Wu, and M. Griffith, "Mitigation Of Blast Effects On Aluminum Foam Protected Masonry Walls," *Trans. Tianjin Univ.*, Vol. 14, No. 1, pp. 558–562, Oct. (2008).
- [5] G. S. Langdon, D. Karagiozova, M. D. Theobald, G. N. Nurick, G. Lu, and R. P. Merrett, "Fracture of Aluminium Foam Core Sacrificial Cladding Subjected to Air-Blast Loading", *Int. J. Impact Eng.*, Vol. 37, No. 6, pp. 638–651, Jun. (2010).
- [6] Y. Li, Z. Li, and F. Han, "Air Flow Resistance and Sound Absorption Behavior of Open-Celled Aluminum Foams with Spherical Cells", *Procedia Mater. Sci.*, Vol. 4, pp. 187–190, Jan. (2014).
- [7] L. J. Gibson and M. F. Ashby, "Cellular Solids: Structure and Properties", Cambridge: Cambridge University Press (1997).
- [8] H. X. Zhu, J. F. Knott, and N. J. Mills, "Analysis of the Elastic Properties of Open-Cell Foams with Tetrakaidecahedral Cells", *J. Mech. Phys. Solids*, Vol. 45, No. 3, pp. 319–343, Mar. (1997).
- [9] W. E. Warren and A. M. Kraynik, "The Linear Elastic Properties of Open-Cell Foams", *J. Appl. Mech.*, Vol. 55, No. 2, pp. 341–346, Jun. (1988).
- [10] O. Sotomayor, "Numerical Modeling of Random 2D and 3D Structural Foams Using Voronoi Diagrams: A Study of Cell Regularity and Compression Response", Thesis, Auburn University (2013).
- [11] O. E. Sotomayor and H. V. Tippur, "Role of Cell Regularity and Relative Density on Elasto-Plastic Compression Response of Random Honeycombs Generated Using Voronoi Diagrams", *Int. J. Solids Struct.*, Vol. 51, No. 21–22, pp. 3776–3786 (2014).
- [12] H. Zhu, J. Hobdell and A. Windle, "Effects of Cell Irregularity on the Elastic Properties of Open-Cell Foams", *Acta Mater.*, Vol. 48, No. 20, pp. 4893–4900, Dec. (2000).
- [13] H. X. Zhu, S. M. Thorpe, and A. H. Windle, "The Effect of Cell Irregularity on the High Strain Compression of 2D Voronoi Honeycombs", *Int. J. Solids Struct.*, Vol. 43, No. 5, pp. 1061–1078, Mar. (2006).
- [14] H. Kanahashi, T. Mukai, T. G. Nieh, T. Aizawa, and K. Higashi, "Effect of Cell Size on the Dynamic Compressive Properties of Open-Celled Aluminum Foams", *Mater. Trans.*, Vol. 43, No. 10, pp. 2548–2553 (2002).
- [15] A. Okabe, Okabe and Atsuyuki, "Spatial Tessellations", *International Encyclopedia of Geography: People, the Earth, Environment and Technology*, Oxford, UK: John Wiley & Sons, Ltd, pp. 1–11 (2017).
- [16] W. L. Martinez, A. R. Martinez, and H. Crc, "Computational Statistics Handbook with Matlab", Vol. 65, No. 1. CRC press (2007).
- [17] M. F. Ashby, "Metal Foams : A Design Guide", Butterworth-Heinemann (2000).
- [18] E. Andrews, G. Gioux, P. Onck, and L. Gibson, "Size Effects in Ductile Cellular Solids. Part i: Experimental Results", *Int. J. Mech. Sci.*, Vol. 43, No. 3, pp. 701–713 (2001).
- [19] O. E. Sotomayor and H. V. Tippur, "Role of Cell Regularity and Relative Density on Elastoplastic Compression Response of 3-D Open-Cell Foam Core Sandwich Structure Generated Using Voronoi Diagrams", *Acta Mater.*, Vol. 78, pp. 301–313, Oct. (2014).
- [20] Y. X. Gan, C. Chen, and Y. P. Shen, "Three-Dimensional Modeling of the Mechanical Property of Linearly Elastic Open Cell Foams", *Int. J. Solids Struct.*, Vol. 42, No. 26, pp. 6628–6642, Dec. (2005).
- [21] H. Si, "Tetgen, a Delaunay-Based Quality Tetrahedral Mesh Generator", *ACM Trans. Math. Softw.*, Vol. 41, No. 2, pp. 1–36, Feb. (2015).

- [22] M. Kutz, "Mechanical Engineers' Handbook, Volume 1: Materials and Engineering Mechanics", 4th ed. Wiley (2015).
- [23] Hibbitt, Karlsson, and Sorensen, "Abaqus/Standard User's Manual", Vol. 1. Hibbitt, Karlsson & Sorensen (2001).
- [24] J. Fish, C. Oskay, R. Fan, and R. Barsoum, "AL 6061-T6-Elastomer Impact Simulations", Report, Rensselaer Polytech. Inst. (2005).

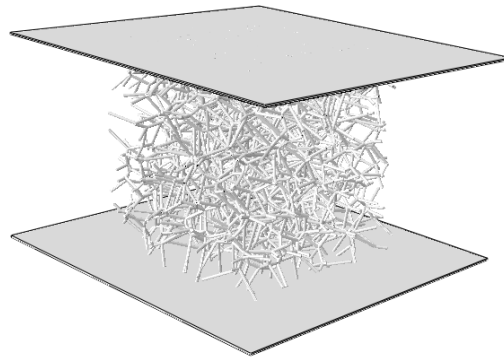


**Fig. 1.** Parts of suggested structural model.

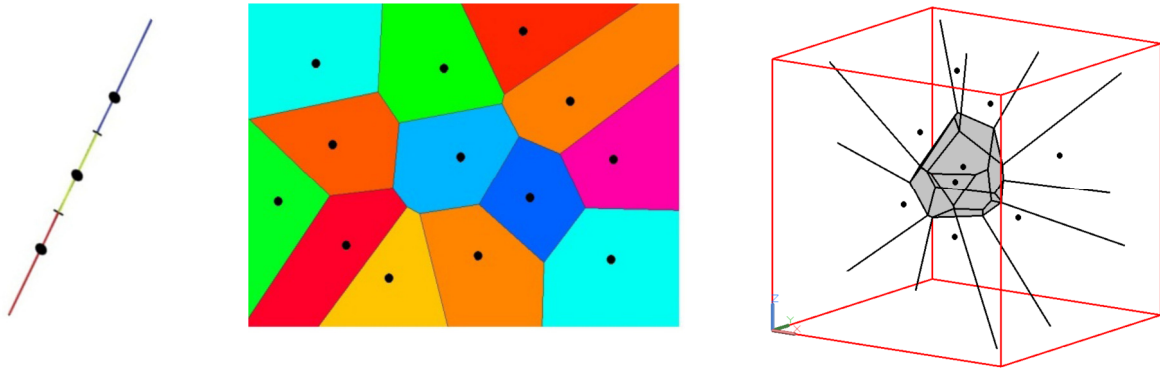


**Fig. 2.** Voronoi diagrams in different dimensions [15].

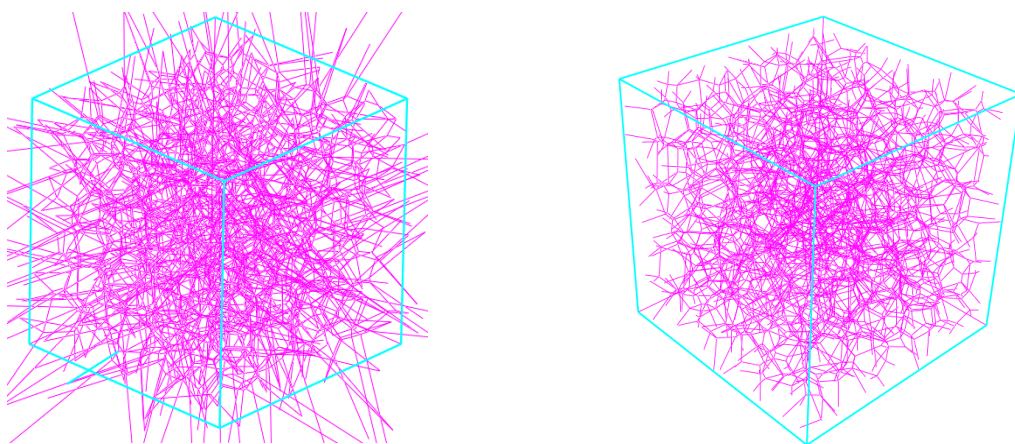


**Fig. 3.** (a) Untrimmed Voronoi cells by boundary planes. (b) Trimmed Voronoi cells by boundary planes.

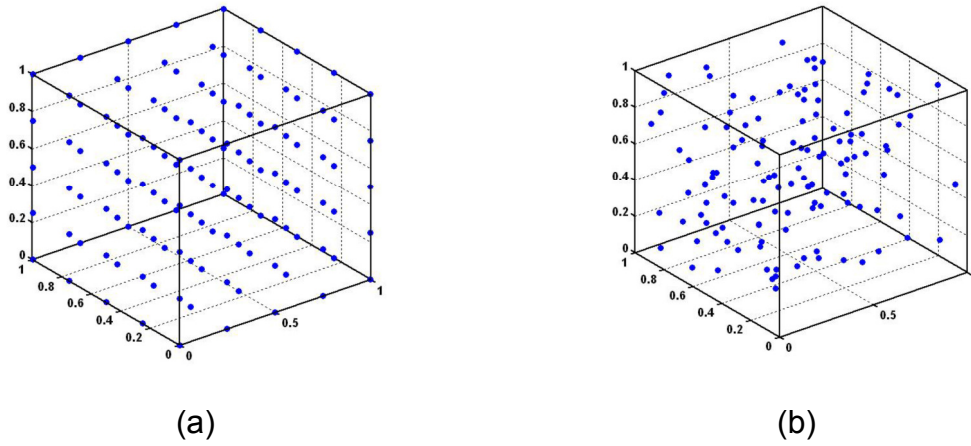


**Fig. 4.** 3D point pattern in a unit cube for  $N = 125$ : (a) seed generated regularly, (b) using SSI method.

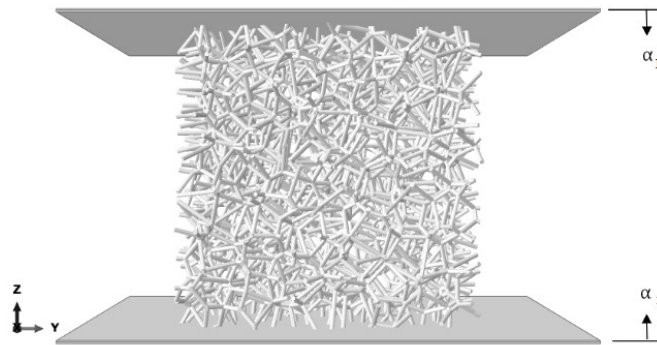


**Fig. 5.** Boundary conditions of suggested structural model.

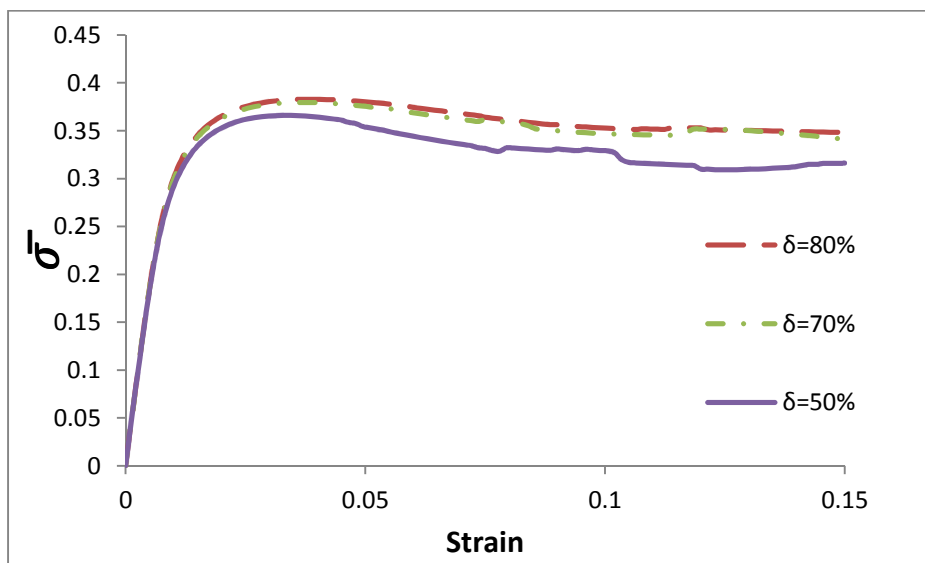


**Fig. 6.** Stress-strain curve of suggested structural model with a relative density 9% at different regularities for strain up to 0.15.

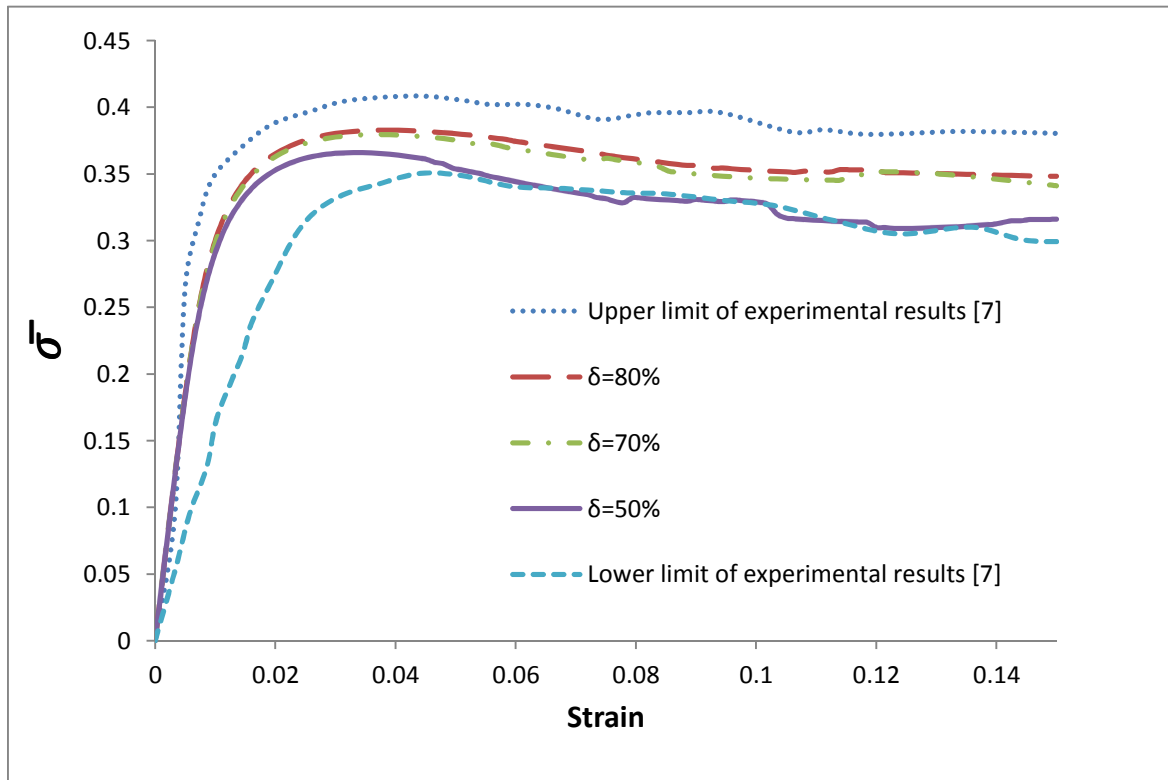


**Fig. 7.** Comparison between predicted normalized stress-strain curves obtained by the present model and measured upper and lower limits of Ref. [7].

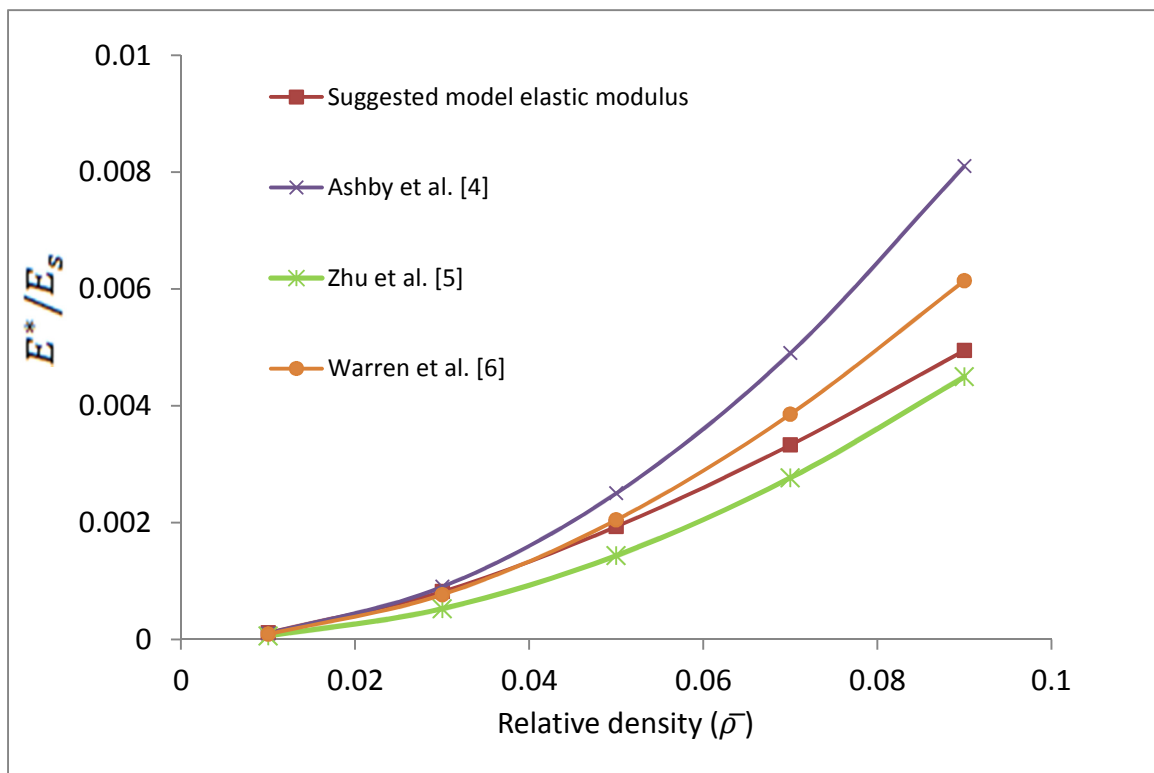


**Fig. 8.** Variation of the elastic modulus of 3D Voronoi foams with relative density.

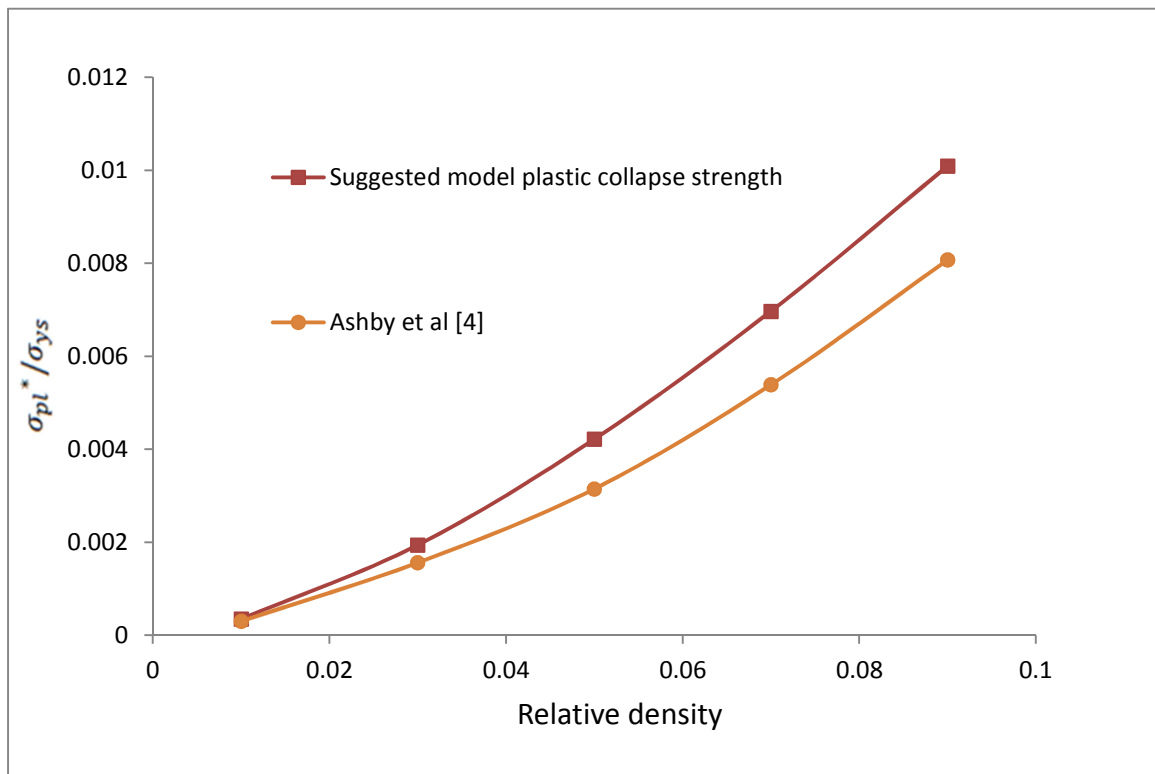


**Fig. 9.** Variation of the plastic collapse strength of 3D Voronoi model with relative density.

**Table 1.** Coefficients of Johnson Cook Constitutive relation [24].

A [MPa]	B [MPa]	c	n	m	$\dot{\epsilon}_0$ [ $s^{-1}$ ]	$\theta_{melt}$ [K]	$\theta_{transition}$ [K]
289.6	203.4	0.011	0.35	1.34	1.0	925.37	294.26